A CAPON-LIKE SPATIAL SPECTRUM ESTIMATOR FOR CORRELATED SOURCES

Richard Abrahamsson, Andreas Jakobsson† and Petre Stoica**

* Dept. of Information Technology, Uppsala University, Box 337, SE-751 05 Uppsala, Sweden
Phone: +46 (0)18 471 7840 , Email: *ra@it.uu.se, ps@it.uu.se*

† Dept. of Electrical Engineering, Karlstad University, SE-651 88 Karlstad, Sweden
Phone: +46 (0)54 700 2330, Email: *andreas.jakobsson@ieee.org*

ABSTRACT

In this paper, we propose a data-adaptive method for estimating the spatial spectrum for correlated and/or coherent sources. The method is reminiscent of the MVDR/Capon beamformer, but yields a multidimensional spatial response with a dimension for each examined source. The estimated directions of arrival (DOA) are given as the points of energy concentration in the multidimensional spatial response. Numerical examples indicate a significant improvement over the standard MVDR/Capon beamformer.

1. INTRODUCTION

The area of sensor array signal processing has received a considerable interest in the recent literature, and numerous algorithms addressing different aspects of the topic have been proposed (see, e.g., [1, 2, 3, 4] and the references therein). Typically, these algorithms exploit the difference in propagation delay recorded at the different sensor array elements to form a parametric or non-parametric spatial spectral estimate. Lately, non-parametric spatial spectrum estimators have received renewed interest, mainly because of their benefit of not explicitly assuming an *a priori* known signal model, which leads to more robustness to variations in the measured signal than parametric counterparts.

A traditional non-parametric method for spatial spectral estimation is to apply a simple beamformer for all directions of interest and use the beamformer outputs to estimate the spatial power spectral distribution. However, such a non-adaptive beamformer suffers from either low resolution or high leakage [3]. The minimum variance distortionless response (MVDR) or Capon beamformer [3, 5] has several desirable properties, and is often applied as a bank of spatial filters when high spatial resolution is desired. The Capon method weighs the array elements in an adaptive manner so as to minimize the beamformer output power while passing signals from a given direction of interest undistorted. This effectively places deep nulls canceling interferences from sources in directions other than the one of interest, resulting in a very high resolution spatial estimate. However, when the impinging wavefronts are correlated or coherent, the Capon beamformer suffers from signal cancellation, causing severe distortions in the spatial spectral estimate [6, 7, 8]. This happens, e.g., when there are multipaths or when smart jammers retrodirect a transmitted signal.

In this paper, we present an extended version of the Capon beamformer that handles correlated and/or coherent signals. The method forms a multidimensional spatial spectral estimate, with a separate dimension for each examined source. Like the Capon beamformer, the proposed method does not require point-like sources or a known noise covariance model in order to perform well; it is only needed that the selected number of examined sources is at least as large as the number of correlated and coherent sources.

This work was partially supported by the Swedish Research Council and Saab Bofors Dynamics. Please address all correspondence to Richard Abrahamsson (*ra@it.uu.se*).

2. PRELIMINARIES

Let $s_p(t)$ denote the pth narrowband signal (narrowband in the sense that the signal bandwidth is much less than the reciprocal of the time it takes for the signal to propagate across the array) impinging from direction θ_p on an M-element sensor array. The array output can be expressed as

$$\mathbf{y}(t) = \sum_{p=1}^{P} \mathbf{a}_{\theta_p} s_p(t) + \mathbf{n}(t),$$

where $\mathbf{a}_\theta$ denotes the array manifold vector for a generic direction of arrival (DOA), θ, $\mathbf{n}(t)$ is a possibly colored additive measurement noise, and P is the number of examined sources. Assuming possibly correlated and/or coherent sources, each signal, $s_j(t)$, can be decomposed as

$$s_j(t) = \frac{E\left\{s_j(t)\overline{s_k(t)}\right\}}{E\left\{\left|s_k(t)\right|^2\right\}} s_k(t) + s_j^{\perp k}(t), \qquad (1)$$

where $E\{\cdot\}$ denotes the expectation operator, $\overline{(\cdot)}$ the complex conjugation, and $s_j^{\perp k}(t)$ is the part of $s_j(t)$ which is uncorrelated with another impinging signal (or interference), $s_k(t)$. Alternatively, assuming constant correlation coefficients between signals over the observation interval, $s_j(t)$ can be written as a linear combination of all interfering signals and a residual term

$$s_j(t) = \sum_{k=1, k\neq j}^{P} \alpha_{j,k} s_k(t) + \tilde{s}_j(t), \qquad (2)$$

for some set of scalars $\alpha_{j,k}$. Here, $\tilde{s}_j(t)$ is the component of $s_j(t)$ which is uncorrelated with all the interfering sources, i.e., $s_k(t), \forall k \neq j$. Hereafter, for simplicity, we limit our interest to pairwise correlated and/or coherent signals, assuming these pairs to be uncorrelated with the remaining source signals. We note that this case is of interest in its own right; pairwise correlated impinging wavefronts occur, e.g., in low angle tracking over sea [9] and in certain GPS applications [10].

However, the following derivation is easily extended to handle the more general case considered in (2). For pairwise correlated/coherent sources, (2) simplifies to, cf. (1),

$$s_j(t) = \alpha_{j,k} s_k(t) + s_j^{\perp k}(t). \tag{3}$$

Note that, if $s_j(t)$ and $s_k(t)$ are uncorrelated, then $\alpha_{j,k} = 0$. On the other hand, if $s_j(t)$ and $s_k(t)$ are fully coherent, then $s_j(t) = \alpha_{j,k} s_k(t)$. To simplify the notation, we hereafter replace $\alpha_{j,k}$ with just α.

3. THE EXTENDED CAPON BEAMFORMER

The Capon beamformer estimates the spatial spectrum for each direction of interest by forming a data-adaptive beampattern focused in the examined direction, say θ, such that deep nulls are placed at directions different from θ that contain power. More specifically, the Capon beamformer minimize the array output power

$$\sigma_\theta^2 = E\left\{|\mathbf{h}^* \mathbf{y}(t)|^2\right\} = \mathbf{h}^* \mathbf{R} \mathbf{h}, \tag{4}$$

with respect to the M-tap array sensor weight vector (the spatial filter), $\mathbf{h}$, subject to the constraint that a signal in the direction of interest should pass undistorted. In (4),

$$\mathbf{R} = E\left\{\mathbf{y}(t)\mathbf{y}^*(t)\right\}$$

is the array output covariance matrix and $(\cdot)^*$ denotes the conjugate transpose. The Capon beamformer design criterion is usually written as

$$\min_{\mathbf{h}} \ \mathbf{h}^* \mathbf{R} \mathbf{h} \quad \text{subject to} \quad \mathbf{h}^* \mathbf{a}_\theta = 1. \tag{5}$$

The solution to (5) is easily found as (see, e.g., [3])

$$\mathbf{h} = \frac{\mathbf{R}^{-1}\mathbf{a}_\theta}{\mathbf{a}_\theta^* \mathbf{R}^{-1} \mathbf{a}_\theta}. \tag{6}$$

In practice, the expectation in (4) is replaced by a sample average, and the sample covariance matrix

$$\hat{\mathbf{R}} = \frac{1}{N} \sum_{t=0}^{N-1} \mathbf{y}(t)\mathbf{y}^*(t)$$

is used in lieu of $\mathbf{R}$, yielding

$$\hat{\sigma}_\theta^2 = \frac{1}{\mathbf{a}_\theta^* \hat{\mathbf{R}}^{-1} \mathbf{a}_\theta} \tag{7}$$

when (6) is inserted in (4). Noting that

$$\begin{aligned} \mathbf{R} - \sigma_\theta^2 \mathbf{a}_\theta \mathbf{a}_\theta^* \geq 0 \Leftrightarrow \\ \mathbf{I} - \sigma^2 \mathbf{R}^{-1/2} \mathbf{a}_\theta \mathbf{a}_\theta^* \mathbf{R}^{-1/2} \geq 0 \Leftrightarrow \\ 1 - \sigma^2 \mathbf{a}_\theta^* \mathbf{R}^{-1} \mathbf{a}_\theta \geq 0 \Leftrightarrow \\ \sigma^2 \leq \frac{1}{\mathbf{a}_\theta^* \mathbf{R}^{-1} \mathbf{a}_\theta}, \end{aligned}$$

where $\mathbf{A} \geq 0$ denotes the positive semidefiniteness of $\mathbf{A}$, the design objective of the Capon beamformer for spatial power spectrum estimation can equivalently be written as [11, 12]

$$\max_{\sigma_\theta^2} \ \sigma_\theta^2 \quad \text{subject to} \quad \mathbf{R} - \sigma_\theta^2 \mathbf{a}_\theta \mathbf{a}_\theta^* \geq 0. \tag{8}$$

The formulation in (8) is intuitively appealing: Finding the maximum power of a signal component at direction θ such that the residual covariance matrix, after removing this signal component, is still positive semi-definite. In the following, we will exploit this formulation to enable estimation of the spatial spectrum for correlated and/or coherent sources.

Under the assumption of pairwise correlated sources, a generic term of the covariance matrix $\mathbf{R}$ from one such pair of signals, say $s_j(t)$ and $s_k(t)$, can be written as (9), on the top of next page, where the signal $s_j(t)$ has been decomposed as in (3), and σ_k^2 and $\sigma_{j\perp k}^2$ are the powers of $s_k(t)$ and the component of $s_j(t)$ which is uncorrelated with $s_k(t)$, respectively. Note that (9) illustrates why the Capon beamformer fails for correlated sources; the coherent part of an interference $s_j(t)$ will create an offset, $\alpha \mathbf{a}_{\theta_j}$, to the steering vector for the signal $s_k(t)$ and hence $s_k(t)$ will appear in the covariance data as if it did *not* come from the examined direction, θ_k. Thus, the data-adaptive filter steered to θ_k will treat the resulting signal (first term on right hand side of (9)) as an interference and will attempt to cancel it out.

Using (8) and (9), we now form the extended Capon beamformer as (10), on the top of next page, where θ_1 denotes the DOA whose power content we are interested in and θ_2 is the DOA of a possible correlated impinging signal. Similarly to (7) that maximizes (8), the solution to (10), for a given α and θ_2, is found as

$$\sigma_{\theta_1}^2 = \frac{1}{\begin{bmatrix} 1 & \alpha^* \end{bmatrix} \begin{bmatrix} \mathbf{a}_{\theta_1}^* \\ \mathbf{a}_{\theta_2}^* \end{bmatrix} \mathbf{R}^{-1} \begin{bmatrix} \mathbf{a}_{\theta_1} & \mathbf{a}_{\theta_2} \end{bmatrix} \begin{bmatrix} 1 \\ \alpha \end{bmatrix}}. \tag{11}$$

Introducing

$$b(\theta_p, \theta_q) = \mathbf{a}_{\theta_p}^* \mathbf{R}^{-1} \mathbf{a}_{\theta_q} \quad \text{for} \quad p, q \in \{1, 2\}.$$

enables us to write (11) as in (12), on the top of the last page of this paper. Thus, the α minimizing (12) (for a particular $\theta_1 \neq \theta_2$) is given as

$$\alpha = -\frac{b^*(\theta_1, \theta_2)}{b(\theta_2, \theta_2)}. \tag{13}$$

Insertion of (12) in (11), using (13), concentrates the optimization in (10) to

$$\sigma_{\theta_1}^2 = \max_{\theta_2} \frac{b(\theta_2, \theta_2)}{b(\theta_1, \theta_1) b(\theta_2, \theta_2) - |b(\theta_1, \theta_2)|^2}. \tag{14}$$

Note that as θ_1 approaches θ_2, i.e., when two possible correlated signals get closer together, $\sigma_{\theta_1}^2$ in (11) will yield very large estimates. This is easily seen from (14), or from the constraint in (10) (when $\mathbf{a}_{\theta_1}$ gets close to $\mathbf{a}_{\theta_2}$, the optimal α will be such that $\mathbf{a}_{\theta_1} + \alpha \mathbf{a}_{\theta_2}$ becomes very small). Thus, care needs to be taken not to evaluate the multidimensional spatial response for a narrow region close to $\theta_1 \approx \theta_2$. If available, prior knowledge of source separation can be exploited to design the width of this narrow region. Worth noting is the fact that one may determine from the cost function in (14) which of the source signals are uncorrelated and which are coherent. The coherent components will appear as peaks mirrored with respect to the line $\theta_1 = \theta_2$, whereas the uncorrelated parts, with $\alpha = 0$, are independent of θ_2 and show up as ridges parallel to the θ_2 axis. See Section 5 for an illustration of this.

$$E\left\{\left[\mathbf{a}_{\theta_k}s_k(t)+\mathbf{a}_{\theta_j}s_j(t)\right]\left[\mathbf{a}_{\theta_k}s_k(t)+\mathbf{a}_{\theta_j}s_j(t)\right]^*\right\}=\sigma_k^2\left[\mathbf{a}_{\theta_k}+\alpha\mathbf{a}_{\theta_j}\right]\left[\mathbf{a}_{\theta_k}+\alpha\mathbf{a}_{\theta_j}\right]^*+\sigma_{j\perp k}^2\mathbf{a}_{\theta_j}\mathbf{a}_{\theta_j}^* \tag{9}$$

$$\max_{\sigma_{\theta_1}^2,\alpha,\theta_2}\sigma_{\theta_1}^2 \quad \text{subject to} \quad \mathbf{R}-\sigma_{\theta_1}^2\left[\mathbf{a}_{\theta_1}+\alpha\mathbf{a}_{\theta_2}\right]\left[\mathbf{a}_{\theta_1}+\alpha\mathbf{a}_{\theta_2}\right]^*\geq 0 \tag{10}$$

4. COMPUTATIONAL COMPLEXITY

For a Uniform Linear Array (ULA), the array manifold vector can be written as

$$\mathbf{a}_\theta=\left[\begin{array}{cccc}1 & e^{i\omega} & \cdots & e^{i\omega(M-1)}\end{array}\right]^T, \tag{15}$$

where $(\cdot)^T$ denotes the transpose,

$$\omega=2\pi\frac{d}{\lambda}\sin(\theta)$$

is the spatial frequency, d is the interelement spacing of the array and λ is the operating wavelength. By sampling the cost function in (14) uniformly on a grid in ω_1, ω_2 (instead of on a grid in θ_1, θ_2), the Fourier-vector form of the array steering vectors, as shown in (15), can be exploited for efficient implementation. Using a grid of $K\times K$ spatial frequency points, the values of $\mathbf{a}_{\theta_p}^*\mathbf{R}^{-1}\mathbf{a}_{\theta_q}$, for $p,q=1,2$, can be computed by first applying the inverse Fast Fourier transform (FFT) to each row of $\mathbf{R}^{-1}$ and then applying the FFT to each column of the result. This results in a total computational complexity of the order $O\{(M+K)K\log_2(K)\}$ which should be compared to $O\{M^2K^2\}$ if direct multiplication is used (or $O\{MK(M+K)\}$ if intermediate data is stored). We note that the computational cost of forming and inverting the sample covariance matrix is of the order of $O\{M^3+MN\}$, which also is the main computational burden for the Capon beamformer if the number of points on the DOA grid, K, is of the same order as M.

5. NUMERICAL EXAMPLE

In the following example, data from a 15-element ULA with half wavelength interelement spacing have been simulated. Wavefronts impinge on the array from angles $-55°$, $-40°$, $0°$, $10°$, $30°$, and $60°$ (as measured from broadside). The impinging signals are simulated as temporally white zero-mean circularly symmetric complex Gaussian sequences. Those from $0°$ and $10°$ are of unit power and uncorrelated, both mutually and with the other signals, whereas the signals from $30°$ and $60°$ are partially correlated with the covariance matrix

$$\left[\begin{array}{cc}\frac{5}{4} & 1\\ 1 & \frac{5}{4}\end{array}\right]$$

and uncorrelated with the rest of the signals. The remaining two signals from the sources located at $-40°$ and $-55°$ are fully coherent with each other (identical up to a constant phase factor), uncorrelated with the other signals, and each having a signal power twice that of the signal impinging from broadside. The noise power in each sensor is 4, i.e., 6 dB above the signal at $\theta_0=0^o$, with the noise being spatially and temporally white and zero-mean circularly symmetric complex Gaussian distributed. The array output is observed for a time period of $N=100$ samples.

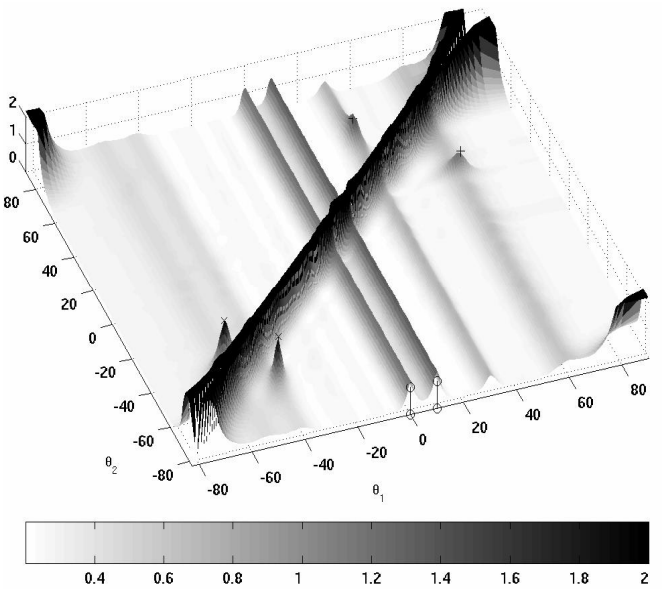

Figure 1: Two dimensional representation of the cost function of the proposed method.

Figure 1 shows the cost function in equation (14) that is to be maximized with respect to the unknown correlated interference direction θ_2. Note how the uncorrelated signals at $0°$ and $10°$ appear as ridges at $\theta_1=0^o$ and $\theta_1=10^o$, both independent of θ_2 (except along the diagonal $\theta_1\approx\theta_2$) as there is no interference that is correlated with these two signals. The true powers of the signals at 0^o and 10^o are indicated by two vertical lines with circles at $\theta_2=-90°$ and their respective DOAs in θ_1. The mutually fully coherent signals at $-40°$ and $-55°$ have their locations and true powers indicated by vertical lines marked with x. Note how the coherent signals appear as peaks at the coordinates of their DOAs in θ_1 and the coherent interference direction in θ_2. Further, the partially correlated signals at $30°$ and $60°$, with the true locations and powers denoted by vertical lines with + signs, appear as superpositions of a θ_2-independent ridge (the uncorrelated component) and peaks at the correlated interference direction in θ_2 (the fully coherent component). In this way, the amount of correlation between signals can be found by observing the peak height in relation to the height of the θ_2-independent ridges. Since the observations are noisy and are made during a limited time, also the fully coherent signals appear to have small uncorrelated components. We note that to enable visualization in Figure 1, the ridge along $\theta_1=\theta_2$ has been truncated.

In Figure 2, the result of the proposed method after maximizing the objective function with respect θ_2, is compared to

$$\begin{bmatrix} 1 & \alpha^* \end{bmatrix} \begin{bmatrix} b(\theta_1,\theta_1) & b(\theta_1,\theta_2) \\ b^*(\theta_1,\theta_2) & b(\theta_2,\theta_2) \end{bmatrix} \begin{bmatrix} 1 \\ \alpha \end{bmatrix} = b(\theta_1,\theta_1) + \alpha^* b(\theta_1,\theta_2)^* + \alpha b(\theta_1,\theta_2) + |\alpha|^2 b(\theta_2,\theta_2)$$

$$= \left| \alpha + \frac{b^*(\theta_1,\theta_2)}{b(\theta_2,\theta_2)} \right|^2 b(\theta_2,\theta_2) + b(\theta_1,\theta_1) - \frac{|b(\theta_1,\theta_2)|^2}{b(\theta_2,\theta_2)} \qquad (12)$$

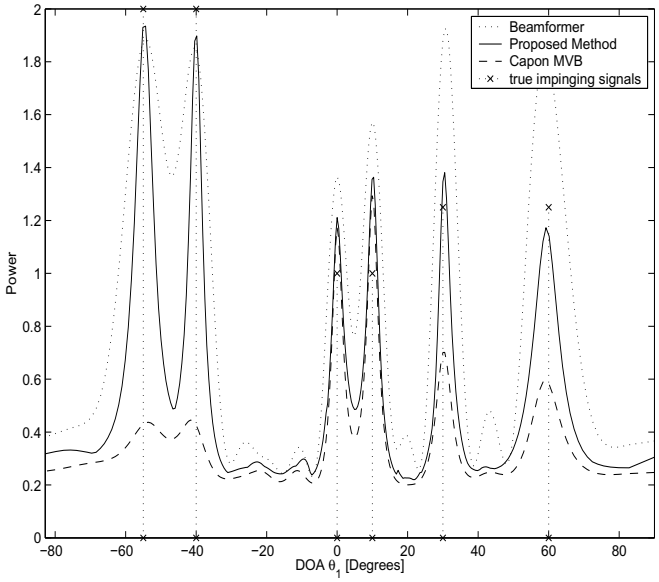

Figure 2: Proposed method (with the ridge at $\theta_1 = \theta_2$ removed) as compared to the standard Capon method and the traditional beamformer

the traditional Capon beamformer estimate. To enable the maximization, the ridge along $\theta_2 \approx \theta_1$ has been excluded prior to the optimization with respect to θ_2. As seen in the figure, the proposed method significantly improves the estimation of the power distribution over different DOAs as compared to the classical Capon beamformer. For reference, the spatial spectral estimate of the traditional data-independent beamformer is also shown. In the figure, the true DOAs and powers of the signals are shown with vertical dotted lines marked with x. Finally, we remark that by using the proposed method we retain the highly desirable resolution and leakage properties of the Capon beamformer even for correlated and/or coherent sources.

6. CONCLUSIONS

In this paper, a Capon-like spatial spectrum estimator has been presented. The proposed algorithm is based on a multidimensional extension of the covariance fitting formulation of the MVDR/Capon beamformer. The extension shows a significant improvement over the MVDR/Capon beamformer when correlated and/or coherent wavefronts are present, while the excellent resolution and leakage properties are retained. Moreover, the multidimensional spatial spectral estimate shows the amount of correlation between signals from different directions. For uniform linear arrays, the computational complexity of the proposed method is not too much higher than that of the Capon method. To simplify notation, only pairwise correlated and/or coherent sources have been considered, with the more general case of several mutually correlated/coherent sources following similarly.

REFERENCES

[1] D. H. Johnson and D. E. Dudgeon, *Array Signal Processing*. Englewood Cliffs, N.J.: Prentice Hall, 1993.

[2] H. Krim and M. Viberg, "Two decades of array signal processing research," *IEEE Signal Processing Magazine*, pp. 67–94, July 1996.

[3] P. Stoica and R. Moses, *Introduction to Spectral Analysis*. Upper Saddle River, NJ: Prentice Hall, 1997.

[4] H. L. Van Trees, *Optimum Array Processing*. No. IV in Detection, Estimation, and Modulation Theory, New York, USA: John Wiley & Sons, 2002.

[5] J. Capon, *"Maximum-Likelihood Spectral Estimation"*. Chapter 5 in *Nonlinear Methods of Spectral Analysis*, 2nd ed., S. Haykin,ed., New York, USA: Springer-Verlag, 1983.

[6] Y. Bresler, V. U. Reddy, and T. Kailath, "Optimum beamforming for coherent signal and interferences," *IEEE Trans. ASSP*, vol. 36, pp. 833–843, June 1988.

[7] T. J. Shan and T. Kailath, "Adaptive beamforming for coherent signals and interference," *IEEE Trans. ASSP*, vol. 33, pp. 527–536, June 1985.

[8] B. Widrow, K. M. Duvall, R. P. Gooch, and W. C. Newman, "Signal cancellation phenomena in adaptive antennas: Causes and cures," *IEEE Trans. Antennas and Propagation*, vol. 30, pp. 469–478, May 1982.

[9] K. Boman and P. Stoica, "Low angle estimation: Models, methods, and bounds," *Digital Signal Processing Rev. Journal*, vol. 11, pp. 35–79, Jan 2001.

[10] R. G. Lorenz and S. P. Boyd, "Robust beamforming in GPS arrays," in *ION National Technical Meeting*, (San Diego, CA), Jan. 28-30 2002.

[11] T. L. Marzetta, "A new interpretation for Capon's maximum likelihood method of frequency-wavenumber spectrum estimation," *IEEE Trans. ASSP*, vol. 31, pp. 446–449, April 1983.

[12] P. Stoica, Z. Wang, and J. Li, "Robust Capon beamforming," *IEEE Signal Processing Letters*, vol. 10, pp. 172–175, June 2003.